Review of Scientific Instruments

Inductively coupled 30 T magnetic field platform for magnetized high-energy-density plasma studies

Cite as: Rev. Sci. Instrum. **89**, 084703 (2018); https://doi.org/10.1063/1.5040756
Submitted: 20 May 2018 . Accepted: 25 July 2018 . Published Online: 13 August 2018

G. Fiksel, R. Backhus, D. H. Barnak, P.-Y. Chang, J. R. Davies, D. Jacobs-Perkins, P. McNally, R. B. Spielman, E. Viges, and R. Betti

Inductively coupled 30 T magnetic field platform for magnetized high-energy-density plasma studies

G. Fiksel,[1,a)] R. Backhus,[2] D. H. Barnak,[3,4] P.-Y. Chang,[5] J. R. Davies,[3,6] D. Jacobs-Perkins,[3] P. McNally,[2] R. B. Spielman,[3] E. Viges,[2] and R. Betti[3,6]
[1]*Center for Ultrafast Optical Science, University of Michigan, Ann Arbor, Michigan 48109, USA*
[2]*Space Research Laboratory, University of Michigan, Ann Arbor, Michigan 48109, USA*
[3]*Laboratory for Laser Energetics, University of Rochester, Rochester, New York 14623, USA*
[4]*Department of Physics and Astronomy, University of Rochester, Rochester, New York 14623, USA*
[5]*Institute of Space and Plasma Sciences, National Cheng Kung University, Tainan, Taiwan*
[6]*Department of Mechanical Engineering, University of Rochester, Rochester, New York 14623, USA*

(Received 20 May 2018; accepted 25 July 2018; published online 13 August 2018)

A pulsed high magnetic field device based on the inductively coupled coil concept [D. H. Barnak *et al.*, Rev. Sci. Instrum. **89**, 033501 (2018)] is described. The device can be used for studying magnetized high-energy-density plasma and is capable of producing a pulsed magnetic field of 30 T inside a single-turn coil with an inner diameter of 6.5 mm and a length of 6.3 mm. The magnetic field is created by discharging a high-voltage capacitor through a multi-turn solenoid, which is inductively coupled to a small single-turn coil. The solenoid electric current pulse of tens of kA and a duration of several μs is inductively transformed to hundreds of kA in the single-turn coil, thus enabling a high magnetic field. Unlike directly driven single-turn systems that require a high-current and low-inductive power supply, the inductively coupled system operates using a relatively low-current power supply with very relaxed requirements for its inductance. This arrangement significantly simplifies the design of the power supply and also makes it possible to place the power supply at a significant distance from the coil. In addition, the device is designed to contain possible wire debris, which makes it attractive for debris-sensitive applications. *Published by AIP Publishing.* https://doi.org/10.1063/1.5040756

I. INTRODUCTION

Over the past decade, there has been considerable interest in magnetized high-energy-density (HED) plasma studies. New and exciting results have been obtained in several HED areas such as direct-drive inertial fusion,[1–4] hohlraum plasma magnetization in indirect-drive inertial fusion,[5] magnetizing liner-imploded plasma in magnetic liner inertial fusion (MagLIF),[6] pair-plasma generation,[7] and the investigation of astrophysical phenomena such as Weibel instability,[8] magnetic reconnection,[9] and collisionless shocks.[10]

To create a high magnetic field for these experiments, a magnetic field platform MIFEDS (magneto-inertial fusion electrical discharge system) has been built at the Laboratory for Laser Energetics (LLE) of the University of Rochester, NY. The original version[11] that was in operation from 2007 to 2011 was later updated[12] to a more flexible system with a larger, 1 μF storage capacitor discharged directly through a multi-turn wire coil wound around a 3D-printed plastic frame. While that system has proved valuable for many experiments cited above, the fields typically achieved are 10–15 T, depending on the coil geometry. The field limitation results from several constraints, including the available stored energy, the circuit and the coil inductance, and practical limits on how small a coil can be while still suitable for the experiment.

Measures underway to overcome these limits include increasing the stored energy, decreasing the circuit inductance, and using thinner wires with improved high-voltage insulation. Another approach proposed initially in the work of Furth *et al.*[13] and discussed in detail for HED applications in the work of Barnak *et al.*[14] is to use a coil coupled to the power supply inductively rather than directly.

II. COIL DESIGN AND POWER SUPPLY SCHEMATIC

A schematic of the inductively coupled coil described in this paper is shown in Fig. 1(a). A power supply drives a current pulse through a multi-turn solenoid inserted into the cylindrical cavity of a conductive shell, thus inducing an oppositely directed current in the shell. The slit through the shell forces current to flow around the tip of the shell, thus inducing a strong magnetic field on the axis of the small hole, hereafter the field-coil. Schematically, the device is arranged in the form of a step-up current transformer with a multi-turn solenoid connected to the power supply as its primary and with the shell and the field-coil being its single-turn secondary. The magnetic field on the field-coil axis can be very high because the field-coil current is proportional to the turn ratio N:1 in the primary and the secondary. An attractive feature of this arrangement is that the field-coil is physically separated from the solenoid, while the latter is fully enclosed inside the shell cavity (for clarity, the flanges covering the sides of the cavity are not shown), thus completely eliminating debris in case of the solenoid's destruction. Finally, the high-current secondary circuit does not contain any electrical contacts and connections that can impede current propagation. A photo of the device is shown in Fig. 1(b).

a)Electronic mail: gfiksel@umich.edu

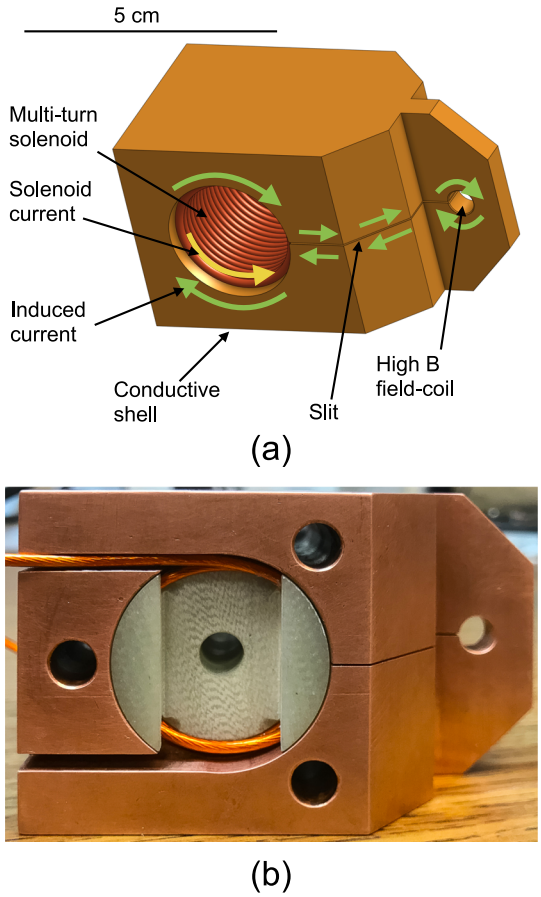

FIG. 1. (a) A schematic of an inductively coupled coil. A power supply drives a pulse of current (yellow arrows) through the solenoid, inducing an oppositely directed current (green arrows) in the conductive shell. The induced current flows around the tip of the shell, thus inducing a strong magnetic field on the axis of the small field-coil. For clarity, the flanges covering the sides of the cavity are not shown. (b) A photo of the device showing the copper shell with the inserted solenoid.

Inductive coupling can be beneficial when the experimental constraints (e.g., laser beams and/or diagnostic access) require the use of a small magnetic coil with a single-digit number of turns. To create a high magnetic field with such a coil requires a high electric current; thus, a power supply with a high stored energy and a low inductance must be used. In general, the latter can only be achieved by placing the power supply very near the coil, which might not always be possible or desirable. On the other hand, inductive coupling requires only a modest current directly from the power supply. In addition, the requirements to the circuit inductance become much more relaxed, thus making possible the placement of the power supply further away from the coil (e.g., outside of the vacuum chamber of the experiment).

For the experiment, we built a power supply consisting of a storage capacitor (GA 33593 50 μF/20 kV) charged with a regulated power supply (Ultravolt 25C24-P250 25 kV/250 W) and discharged through the solenoid via a triggered spark gap (Excelitas GP-14B). The spark gap is triggered by a 30 kV/100 ns pulse provided by a custom-made NorthStar HV pulse generator. The output of the power supply is connected to the solenoid by a 5 m-long bundle of four parallel

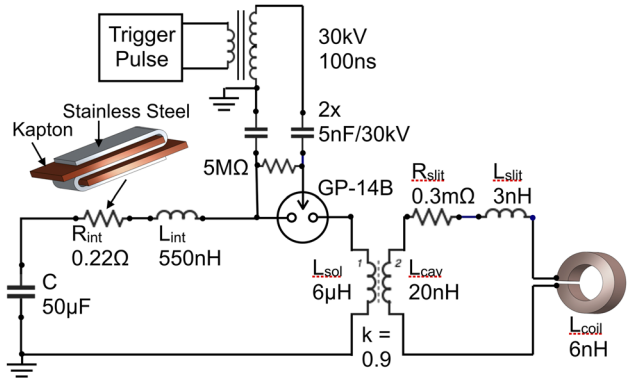

FIG. 2. A simplified circuit schematic. R_{int} and L_{int} are the lumped internal resistance and inductance of the power supply. L_{sol} and L_{cav} are the inductances of the solenoid and the cylindrical cavity in the shell. R_{slit} and L_{slit} are the resistance and inductance of the slit in the shell, and L_{coil} is the inductance of a cylindrical field-coil with a diameter of 6.5 mm and a length of 6.3 mm. The solenoid and the cavity are coupled with a transformer with a coupling factor $k = 0.9$. These circuit parameters are estimated assuming one-skin-length current penetration into the conductors using room temperature resistivity.

high-voltage, low-inductance 60 nH/m cables from Dielectric Sciences, Inc. To keep the current from ringing, a custom-built low-inductive 0.2 Ω shaping resistor (shown in Fig. 2) is inserted in series with the output cables. The resistor is made with a strip of stainless steel foil with a length of 2.2 m, a width of 5 cm, and a thickness of 0.15 mm. The strip is folded multiple times and insulated with 0.1 mm-thick Kapton sheets inserted between the folds. The discharge current is monitored with a Pearson current monitor (Pearson-Electronics 1330). The internal resistance of the power supply is 0.22 Ω, and its inductance is 550 nH, including all the circuit elements and the output cables. The power supply is capable of providing a short-circuit current of 67 kA at a capacitor charge of 20 kV.

For the described set of results, the solenoid with an outer diameter of 32 mm and a length of 50 mm is formed by 22 turns of a Kapton-insulated wire (Accu-Glass Products, Inc.) with a size of AWG14 (core diameter 1.6 mm) and is

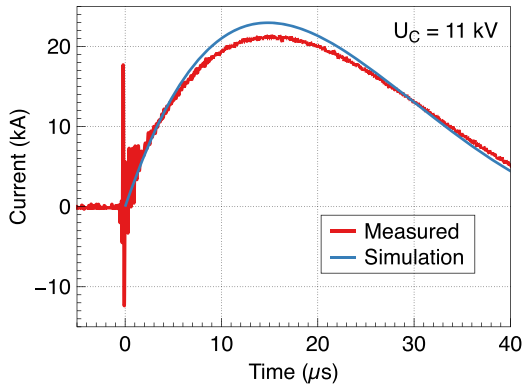

FIG. 3. Comparison of the measured and simulated solenoid current using the circuit parameters in Fig. 2. The capacitor voltage was set at $U_C = 11$ kV. Current pulse simulation uses room temperature resistivity assuming one-skin-length current penetration into the conductors.

tightly fit inside the cavity to maximize the inductive coupling. The field-coil has a diameter of 6.53 mm and a length of 6.35 mm. This geometry can be optimized according to the specific requirements of an experiment.

A simplified circuit schematic is shown in Fig. 2. Figure 3 illustrates a very good agreement between the circuit simulations and measurements.

III. TEST RESULTS AND COMPARISON TO SIMULATIONS

To further develop predictive capabilities, the coil operation was modeled using the COMSOL Multiphysics® package that allows for the most complete and accurate modeling and includes such important physics as current diffusion (skin effect), heat transport, and temperature-dependent resistivity. A comparison of measured and simulated magnetic field waveforms shown in Fig. 4 illustrates excellent agreement between measurements and simulations. Figure 5 shows the distribution of the field coil current density across the coil cross section. Due to the skin effect, the current is peaked very near the coil inner surface, and the total surface-integrated coil current is I_{coil} = 220 kA.

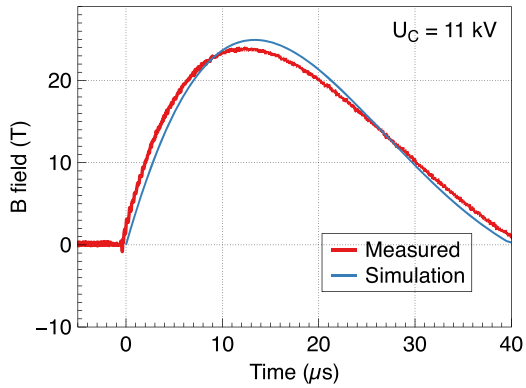

FIG. 4. Comparison of the measured magnetic field (red curve) and the COMSOL simulation (blue curve). The capacitor voltage was set at U_C = 11 kV. Magnetic filed simulation includes multiphysics of the field-coil, excluding time-dependent deformation of the shell and field-coil.

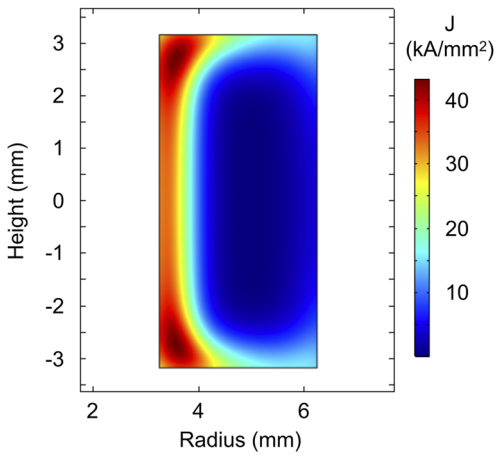

FIG. 5. A map of the current density across the field coil cross section. The total surface-integrated coil current is I_{coil} = 220 kA.

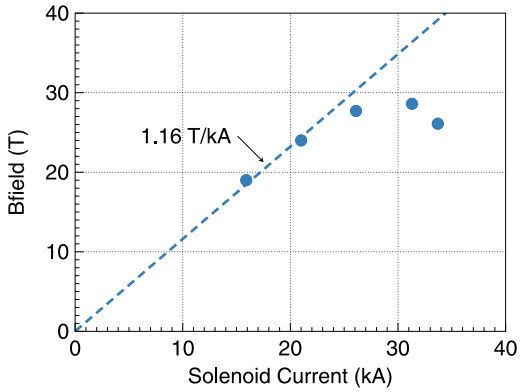

FIG. 6. Dependence of the field-coil magnetic field on the solenoid current. Circles correspond to experimental data. The dashed line corresponds to a linear fit to indicate the rate of magnetic field change with the current.

The dependence of the field-coil peak magnetic field on the solenoid current is shown in Fig. 6. The magnetic field was measured using a calibrated B-dot probe made of several turns of a thin AWG 18 magnet wire. A peak field of $B \approx 30$ T at the field-coil center was obtained at a solenoid current of ≈30 kA. However, the rate at which the field changes with the current falls (the B-vs-I curve deviates from the initially linear dependence), and at a higher solenoid current, it even becomes negative! The reason for this behavior is increased field-coil size resulting from the high magnetic forces. Had the field-coil remained the same size, the field should have been about 40 T as indicated by the extrapolation of the linear fit.

IV. A SIMPLE MODEL OF COIL EXPANSION

An accurate modeling of the coil expansion is rather complicated given the large electromagnetic forces. The peak of magnetic pressure $P_M = B^2/2\mu_0$ is of the order of 360 MPa at B = 30 T and that exceeds the copper tensile stress of ~200 MPa. The regime of elastic deformation ends after the tensile stress limit has been reached, and given the copper Young's module of 100 GPa, it happens very early into the pulse at a small strain of about 0.002 mm/mm. After that, the coil expansion is governed by very non-linear processes especially if the geometry, material heating, current diffusion, etc., are taken into account.

However, it is instructive to construct an approximate model of the coil expansion to estimate its magnitude and scaling. Given that the profile of the current in the field coil is very narrow and is peaked at the inner coil surface (see Fig. 5), the electromagnetic force action can be approximated by that of a piston applying an outward pressure of $P_M = B^2/2\mu_0$ to the field coil inner surface. An upper bound of the coil expansion can be obtained by neglecting the deformation forces, so the magnetic force is balanced by the coil material acceleration,

$$P_M = d(mv)/dt, \tag{1}$$

and the buildup of the moving coil material is described by an incompressible 1-D "snow-plow" model,

$$m = \rho x. \tag{2}$$

Here, m, $v = dx/dt$, and x are the mass (per unit area), velocity, and radial displacement of the moving copper layer, and ρ is the specific density of the material.

Approximating the magnetic field waveform by $B = B_0 \sin(\pi t/T_{1/2})$ ($T_{1/2}$ is a half-period of the modulation) results in an expression for the material displacement δ by the end of the current pulse,

$$\delta = 0.5 B_0 T_{1/2} (\rho \mu_0)^{-1/2}. \tag{3}$$

For $B_0 = 30$ T and $T_{1/2} = 30$ μs, $\delta \approx 4$ mm. These estimates agree, within a factor of 2, with the actual coil expansion, which is quite reasonable given the model approximations.

A possible improvement could be reduction in the pulse duration, replacement of the copper shell material to a material with a higher tensile stress and/or higher density (e.g., BeCu or W), and/or construction of a reinforcing outer shell to contain the shell expansion. Exploration of acceptable methods, as well as a more accurate treatment of the coil expansion, is a subject of future work.

V. CONCLUSIONS

To conclude, a high magnetic field platform based on inductive coupling has been developed and tested. The device is capable of generating a pulse of magnetic field of 30 T and a duration of 10 μs and can be used in many high energy density plasma experiments requiring plasma magnetization.

Currently, the field magnitude appears to be limited by the structural strength of the field-coil material (copper), and future work will explore ways of circumventing this limitation. In addition, even in case of complete solenoid destruction, its debris is fully contained, which makes this coil attractive for debris-sensitive applications.

ACKNOWLEDGMENTS

This work has been supported in part by the University of Michigan research Grant No. U051442 and the U.S. Department of Energy OFES Award No. DE-SC0016258.

[1]O. V. Gotchev, P. Y. Chang, J. P. Knauer, D. D. Meyerhofer, O. Polomarov, J. Frenje, C. K. Li, M. J.-E. Manuel, R. D. Petrasso, J. R. Rygg, F. H. Seguin, and R. Betti, Phys. Rev. Lett. **103**, 215004 (2009).
[2]J. P. Knauer, O. V. Gotchev, P. Y. Chang, D. D. Meyerhofer, O. Polomarov, R. Betti, J. A. Frenje, C. K. Li, M. J.-E. Manuel, R. D. Petrasso, J. R. Rygg, and F. H. Séguin, Phys. Plasmas **17**, 056318 (2010).
[3]P.-Y. Chang, G. Fiksel, M. Hohenberger, J. P. Knauer, R. Betti, F. J. Marshall, D. D. Meyerhofer, F. H. Seguin, and R. D. Petrasso, Phys. Rev. Lett. **107**, 035006 (2011).
[4]M. Hohenberger, P. Y. Chang, G. Fiksel, J. P. Knauer, R. Betti, F. J. Marshall, D. D. Meyerhofer, F. H. Seguin, and R. D. Petrasso, Phys. Plasmas **19**, 056306 (2012).
[5]D. S. Montgomery, B. J. Albright, D. H. Barnak, P. Y. Chang, J. R. Davies, G. Fiksel, D. H. Froula, J. L. Kline, M. J. MacDonald, A. B. Sefkow, L. Yin, and R. Betti, Phys. Plasmas **22**, 010703 (2015).
[6]S. A. Slutz, M. C. Herrmann, R. A. Vesey, A. B. Sefkow, D. B. Sinars, D. C. Rovang, K. J. Peterson, and M. E. Cuneo, Phys. Plasmas **17**, 056303 (2010).
[7]H. Chen, G. Fiksel, D. Barnak, P. Y. Chang, R. F. Heeter, A. Link, and D. D. Meyerhofer, Phys. Plasmas **21**, 040703 (2014).
[8]W. Fox, G. Fiksel, A. Bhattacharjee, P. Y. Chang, K. Germaschewski, S. X. Hu, and P. M. Nilson, Phys. Rev. Lett. **111**, 225002 (2013).
[9]G. Fiksel, W. Fox, A. Bhattacharjee, D. H. Barnak, P. Y. Chang, K. Germaschewski, S. X. Hu, and P. M. Nilson, Phys. Rev. Lett. **113**, 105003 (2014).
[10]D. B. Schaeffer, W. Fox, D. Haberberger, G. Fiksel, A. Bhattacharjee, D. H. Barnak, S. X. Hu, and K. Germaschewski, Phys. Rev. Lett. **119**, 025001 (2017).
[11]O. V. Gotchev, J. P. Knauer, P. Y. Chang, N. W. Jang, M. J. Shoup III, D. D. Meyerhofer, and R. Betti, Rev. Sci. Instrum. **80**, 043504 (2009).
[12]G. Fiksel, A. Agliata, D. Barnak, G. Brent, P. Y. Chang, L. Folnsbee, G. Gates, D. Hasset, D. Lonobile, J. Magoon, D. Mastrosimone, M. J. Shoup III, and R. Betti, Rev. Sci. Instrum. **86**, 016105 (2015).
[13]H. P. Furth, M. A. Levine, and R. W. Waniek, Rev. Sci. Instrum. **28**, 949 (1957).
[14]D. H. Barnak, J. R. Davies, G. Fiksel, P. Y. Chang, E. Zabir, and R. Betti, Rev. Sci. Instrum. **89**, 033501 (2018).